JOURNAL OF Applied Polymer SCIENCE

Thermally stable bromobutyl rubber with a high crosslinking density based on a 4,4′-bismaleimidodiphenylmethane curing agent

Shibulal Gopi Sathi, Jun Yeol Jang, Kwang-Un Jeong, Changwoon Nah
Haptic Polymer Composite Research Team and Department of Polymer Nano Science and Technology, Chonbuk National University, 567 Baekje-Daero, Jeonju 561-756, Republic of Korea
Correspondence to: C. Nah (E-mail: cnah@jbnu.ac.kr)

ABSTRACT: The development of thermally stable bromobutyl rubbers has been a challenge in rubber chemistry and engineering. In this circumstance, 4,4′-bismaleimidodiphenylmethane (BMI) was newly applied as a novel crosslinking agent for thermally stable brominated isobutylene–isoprene rubber (BIIR) with a high crosslinking density. With oscillating disk rheometry and differential scanning calorimetry, the curing characteristics of BIIR were systematically investigated with respect to the content of BMI. We found that BMI alone could crosslink BIIR at higher temperature, and a corresponding possible chemical reaction mechanism was proposed. With the introduction of zinc oxide, the curing reaction of BIIR with BMI was significantly accelerated, and the resulting vulcanizate provided a higher state of curing with excellent overcure reversion stability even at a temperature of 190 °C for 2 h. The content of the dicumyl peroxide (DCP) reaction accelerator was also optimized to be BMI/DCP = 1:0.05 on the basis of considerations of the curing rate, scorch safety, maximum rheometric torque, and reversion resistance at 160 °C. Compared with the conventional sulfur-cured BIIR, the BMI-cured BIIR exhibited a higher crosslinking density with a superior low compression set property at elevated temperatures and an excellent thermal stability. © 2016 Wiley Periodicals, Inc. J. Appl. Polym. Sci. **2016**, *133*, 44092.

KEYWORDS: crosslinking; elastomers; rubber

Received 20 February 2016; accepted 17 June 2016
DOI: 10.1002/app.44092

INTRODUCTION

Isobutylene–isoprene rubber (IIR) is an isobutylene-based random copolymer containing 1–3 mol of isoprene; this can provide reactive sites during crosslinking reactions. The low content of isoprene in IIR can cause unsaturated vulcanization. Because of the exceptional air impermeability originating from the sluggish movements of methyl groups of isobutylene segments, butyl rubbers have mainly been applied as elastomeric materials in inner tubes and tire liners. The high loss modulus, extended fatigue life, and oxidative stability of butyl rubbers have made them favorite materials in mechanical damping applications.[1,2] Because of the carbon–carbon double bonds and the active allylic functionality from isoprene, IIR can be crosslinked with sulfur, quinone dioxime, or phenolic resins.[3,4] Even though the sulfur-cured system has often been accepted for the vulcanization of IIR, the sulfur-cured system exhibits poor vulcanizate properties and low curing compatibility with other diene-based elastomers, such as polybutadiene or styrene–butadiene rubber, mainly because of the low level of unsaturation. Moreover, IIR does not undergo free-radical crosslinking because of macroradical fragmentations in the conventional curing environment.[1]

To overcome these limitations, the halogenations of IIR in hexane solution have been investigated since the 1950s. With NMR spectroscopy, Vukov and coworkers[5,6] found that the major microstructure of bromobutyl rubber is exomethylene bromobutyl with bromomethyl butyl as the minor isomer. By investigating the thermal stability of brominated butyl rubber, Parent and coworkers[7,8] reported the fact that at elevated temperatures (at vulcanization temperatures), exomethylene isomers of bromobutyl rubber rearranged to the more thermodynamically stable bromomethyl isomers followed by dehydrobromination to provide a butyl rubber with a conjugated diene structure. Because of the presence of the active allylic bromide functionality, the bromobutyl rubbers significantly improved the rate of sulfur vulcanization and enhanced the curing compatibility with unsaturated elastomers. Moreover, the exomethylene allylic bromide, as depicted in Figure 1(a) within the brominated isobutylene–isoprene rubber (BIIR), allowed it to be crosslinked with zinc oxide (ZnO).[9] When BIIR was reacted with ZnO at high temperatures, the exomethylene isomer of the bromobutyl rubber produced the conjugated diene butyl via the dehydrobromination reaction.[9] The generated HBr further reacted with ZnO to form $ZnBr_2$, which acted as an initiator for the cationic

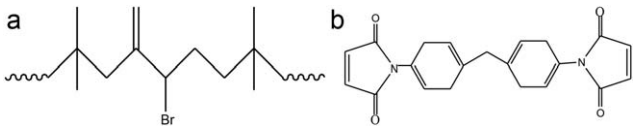

Figure 1. Chemical structures of (a) BMI and (b) bromobutyl rubber (BIIR) with exomethylene allylic bromide functionality.

crosslinking of the exomethylene isomer of BIIR with the formation of a stable carbon–carbon bond.[9] Because the formation of conjugated diene butyl functions is predominant, the number of available sites for the ZnO vulcanization was low, and the crosslinking density offered by ZnO vulcanization was relatively poor. To avoid ZnO in pharmaceutical applications, hexamethylene diamine carbamate was applied to crosslink the allylic bromide functions of bromobutyl rubber.[1] Apart from the enhanced curing activity and the diversity in curing chemistry, halobutyl rubbers can be chemically modified to introduce various functional groups; this is very difficult in butyl rubber itself because of its poor chemical reactivity.[10–12] Over the past decade, the Whitney research group has reported various nucleophilic substitution reactions of BIIR to introduce amine, ester, ether, sulfur, ammonium, and phosphonium salt functionalities onto butyl rubbers.[13–17] Recently, Amit *et al.*[18] developed a self-healing elastomeric material based on BIIR through the chemical modification of BIIR with butyl imidazolium into an imidazolium-modified BIIR.

Although butyl rubbers undergo chain breakdown reactions under the influence of peroxide, they can be crosslinked with peroxide when suitable coagents are presented together. Here, coagents refer to multifunctional organic molecules, which are highly reactive to free radicals. The applied coagents in the peroxide-curing system can enhance the crosslinking density. Molecules containing maleimide groups, acrylate groups, and allylic groups have been used as coagents for peroxide vulcanization.[19] For instance, Sudo *et al.*[20] cured butyl rubber with 0.5–2.5 mol % isoprene in the presence of a bismaleimide coagent. Resendes *et al.*[21] developed a formulation based on a higher isoprene content butyl rubber with dicumyl peroxide (DCP) and *N,N′-m*-phenylene dimaleimide with a curing yield that was superior to those generated by Sudo *et al.* It was also reported by Ho and Steevenz[22] that chlorobutyl rubber could be crosslinked with various types of bismaleimide in the presence of ZnO via a Diels–Alder reaction. They claimed that aromatic bismaleimide gave a higher degree of crosslinking than its aliphatic analogue. Recently, Takenaka *et al.*[23] reported the synthesis of a peroxide-curable butyl rubber via the Suzuki–Miyaura coupling reaction of chlorinated and brominated butyl rubber with 4-vinylphenylboronic acid.

To our knowledge, 4,4′-bismaleimidodiphenylmethane (BMI) has not been considered as a crosslinking agent for BIIR. In this research, we explored the possibility of BMI as a crosslinking agent in the presence of DCP or ZnO for the development of a thermally stable BIIR with a high crosslinking density. The curing characteristics and possible reaction mechanisms were investigated by a combination of oscillating disc rheometry and isothermal differential scanning calorimetry (DSC) analyses. The mechanical properties of the BIIR cured with BMI were systematically investigated with respect to the contents of DCP and ZnO at the optimized time and temperature.

EXPERIMENTAL

Materials

IIR [Lanxess X Butyl RB 301, unsaturation = 1.85 ± 0.20 mol %, Mooney viscosity ML(1+8) at 125 °C = 51 ± 5] and BIIR [Lanxess X Butyl BBX2, bromine content = 1.8 ± 0.20 mol %, Mooney viscosity $ML_{(1+8)}$ at 125 °C = 46 ± 4] were used as the base elastomers. Bismaleimide (BMI; purity = 99.2%, New Century Holding Group Co., Ltd., China) was used as the major curing agent in this study. The chemical structure of the bismaleimide is shown in Figure 1(b). Other ingredients, such as DCP, sulfur, 2-mercaptobezothiazole (MBTS), stearic acid, and ZnO, were purchased from Sigma-Aldrich.

Preparation of the Rubber Compounds

The formulations of rubber compounds used to explore the curing behavior of BMI in BIIR are displayed in Table I. Compound A was a typical sulfur vulcanization system for BIIR used in inner tire liners. Compound B was used to understand the effect of various concentrations of BMI on the curing dynamics and also to fix the optimum level of BMI. Compounds C and D were used to understand the effects of ZnO and DCP on the curing efficiency of BMI with BIIR. Compound E was used to evaluate the synergistic effect of the optimum concentrations of DCP and ZnO on the curing characteristics of BMI with BIIR. All of the compounds were prepared with an internal mixer (Banbury-type mixer, Nam Yang Corp., South Korea) The pristine BIIR was masticated at 60 °C under 35 rpm for 2 min. To

Table I. Formulation of the BIIR Compounds for Curing

	Compound (phr)				
Composition	A	B	C	D	E
BIIR	100	100	100	100	100
Sulfur	0.5	—	—	—	—
MBTS	1.3	—	—	—	—
ZnO	3.0	—	2.5:5	—	2.5
Stearic acid	1.0	—	—	—	—
BMI	—	1:3:5:10	5	5	5
DCP	—	—	—	0.25:0.5:1:2:3	0.25

this, BMI (for compounds B) and BMI plus ZnO (for compounds C) were added, and we continued mixing under the same rotor speed and temperature for 5 min more. For compounds D and E, the DCP was added at the 7th minute, and mixing was continued for another 2 min more. After mixing, the compound was discharged and then molded into a 2-mm sheet at a constant pressure of 25 tons with a compression molding press (CMv 50H-15-CLPX, Carver) for the respective curing time obtained from the rheometry curing data.

Characterization

Curing Characteristics. The maximum torque, minimum torque, difference between the maximum and minimum torques (ΔM), scorch time (T_{S2}), and optimum curing time (T_{90}; i.e., the time required for the torque to reach 90% of the maximum torque) of the rubber compounds were determined from the curing curves generated with an oscillating disk rheometer (Alpha Technologies) at various vulcanization temperatures. The curing rate index, a measure of the rate of curing, was calculated as follows:

$$\text{Curing rate index} = 100/(T_{90} - T_{S2}) \tag{1}$$

Thermal Analysis. DSC analysis was performed on a TA Instruments Q10 to understand the curing behavior. The measurements were carried out with the uncured samples under isothermal conditions at four different temperatures: 160,170,180, and 190 °C. Thermogravimetric analysis (TGA) was also carried out with a TA Instruments Q50 instrument to understand the thermal degradation behavior of the sulfur-cured BIIR and the BMI-cured BIIR. The samples were heated from room temperature to 600 °C at a heating rate of 10 °C/min under a nitrogen atmosphere.

Crosslinking Density Measurements. The degree of crosslinking was determined by the equilibrium swelling method and from the stress–strain plot with the Mooney–Rivlin equation. To determine the crosslinking density via the equilibrium swelling method, samples 25 mm in length by 25 mm in width by 2 mm in thickness were swollen in a dodecane solvent at room temperature until equilibrium was reached. The weights of the swollen samples were then recorded, and the degree of swelling (Q_r) was estimated with the following equation:

$$Q_r = \frac{W_{sw} - W_i}{W_i} \tag{2}$$

where W_i is the initial dry weight and W_{sw} is the swollen weight of the specimen.

The crosslinking density of the samples (n) was then calculated quantitatively with the Flory–Rehner equation[24]:

$$-[\ln(1-\upsilon_2)+\upsilon_2+\chi_1\upsilon_2^2] = \upsilon_1 n^1 \left[\upsilon_2^{1/3} - \frac{\upsilon_2}{2}\right] \tag{3}$$

where ν_2 is the polymer volume fraction in the swollen state ($1/Q_r$), ν_1 is the molar volume of the solvent (227.11 mL/mol for dodecane at room temperature), and χ_1 is the coefficient of the interaction between the polymer and the solvent (0.34). This was determined with the Bristow–Watson equation:[25]

$$\chi_1 = \beta_1 + (\upsilon_s/RT)(\delta_s - \delta_p)^2 \tag{4}$$

where β_1 is the lattice constant (typically, 0.34), ν_s is the volume of solvent per molecule, R is the gas constant, T is the absolute temperature, and δ_p and δ_s are the solubility parameters of BIIR [7.8 $(cal/cc)^{1/2}$] and the solvent dodecane [8.0 $(cal/cc)^{1/2}$], respectively.[26]

To determine the crosslinking density via the Mooney–Rivlin equation,[27–29] a plot of the reduced stress against the reciprocal of the extension ratio ($1/\lambda$) was made from the respective stress–strain values. The intercept obtained by the fitting of a straight line was taken for the crosslinking density measurement.

The Mooney–Rivlin equation was as follows:

$$\text{Reduced stress} = \frac{\sigma}{2\left(\lambda - \frac{1}{\lambda^2}\right)} = C_1 + \frac{C_2}{\lambda} \tag{5}$$

where σ is the nominal tensile stress (force divided by the undeformed cross-sectional area of the sample), λ is the extension ratio (the ratio of the final length to the initial length). The characterizing constants, C_1 (intercept) and C_2 (slope), were obtained from the Mooney–Rivilin plot of the reduced stress versus $1/\lambda$. It is well known that the value of C_1 is connected to the physically manifested crosslinking density (n_{phy}) as follows:

$$n_{phy} = \frac{C_1}{RT} \tag{6}$$

where R is the universal gas constant (8.314 J mol^{-1} K^{-1}) and T is room temperature (298 K).

Mechanical Properties. ***Tensile testing.*** The tensile test was carried out with an LRX Plus machine (Lloyd Instruments, United Kingdom) in accordance with ASTM D 412. Dumbbell-shaped specimens were prepared from molded sheets of the samples and tested at a crosshead speed of 500 mm/min at room temperature. Six samples were taken for each compound, and their averages with standard deviations are reported.

Hardness testing. Round samples 6 mm in thickness and 10 mm in diameter with smooth and uniform surfaces were used to measure the indentation hardness of the cured samples with a Shore A hardness tester (Asker, Kobunishi Keiki Co., Ltd.) per ASTM D 2240. Through the application of a constant force without any disturbances for a specific time, indentations were made in various positions. Ten readings were taken from different areas of the testing samples, and the average value was estimated.

Compression set. The compression set of the vulcanized compounds were determined with cylindrical specimens (12.5 mm in height and 29 mm in diameter) through the application of 25% compression. The samples were kept in an air oven at the testing temperature for 72 h according to ASTM D 395. The test was performed at two different temperatures, 70 and 100 °C. At the end of the test, the samples were taken out and allowed to cool at room temperature for 30 min, and the final height was measured. The compression set was then calculated with the following equation:

$$\text{Compression set (\%)} = \frac{H_0 - H_1}{H_0 - H_s} \times 100 \tag{7}$$

where H_0 and H_1 are the initial and final heights of the specimen, respectively, and H_s is the height of the spacer bar used.

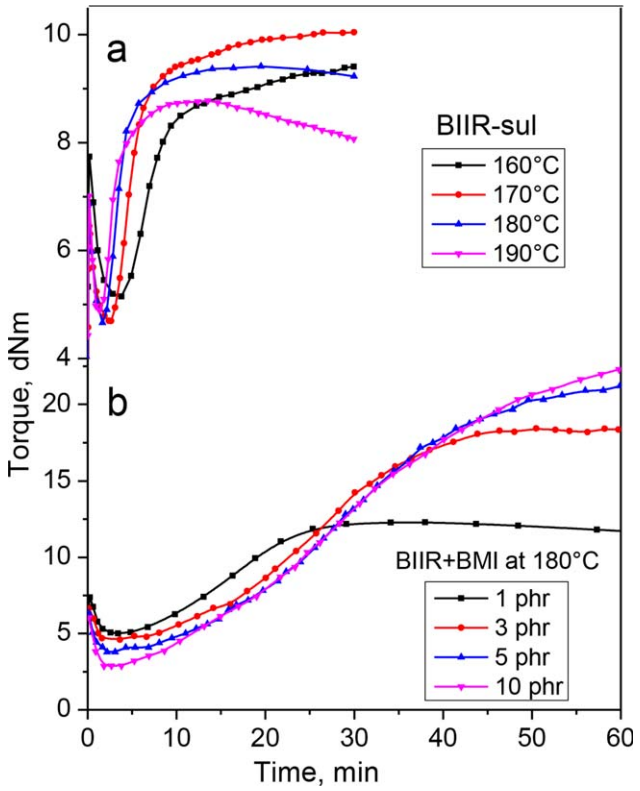

Figure 2. Curing characteristics of (a) BIIR-sul at various temperatures and (b) BIIR with different concentrations of BMI at 180 °C. [Color figure can be viewed in the online issue, which is available at wileyonlinelibrary.com.]

RESULTS AND DISCUSSION

Curing Characteristics of BIIR with BMI

As a first step toward understanding the curing behavior of BIIR with BMI and also to know how this bismaleimide curing behavior is different from the well-established sulfur-accelerated curing system, the curing profiles of unfilled BIIR with a typical sulfur-curing system and with BMI were generated with an oscillating disc rheometer. Figure 2(a,b) presents the curing dynamics of compound A [BIIR with a sulfur-accelerated system (BIIR-sul) at 160, 170, 180, and 190 °C for 30 min] and compound B (BIIR with different concentrations of BMI from 1 to 10 phr at 180 °C for 1 h). Table II represents the curing characteristics of compounds A and B. The sulfur-curing system gave a balance of scorch safety and curing rate at 160 °C. However, it exhibited a reversion tendency at 180 °C. This was presumably due to the breaking of the polysulfide linkages present in the vulcanizate at high temperature.[30] On the contrary, the crosslinking of BIIR with BMI showed a slow curing profile (low curing rate) with increased rheometric torque (high state of curing). For instance, the curing of BIIR with 1-phr BMI increased ΔM to about 55% with excellent stability to overcure reversion at 180 °C up to 1 h. ΔM was further increased to 265% with 5-phr BMI and to 300% with 10-phr BMI. As the concentration of BMI increased, it took a longer time to reach a curing plateau (equilibrium torque). For instance, it took about 30 min for 1-phr BMI and 47 min for 3-phr BMI to reach the curing plateau region. With 5-phr BMI and beyond that, it never showed a curing plateau but continued to increase the torque indefinitely up to a reaction time of 1 h.

Proposed Crosslinking Mechanism between BIIR and BMI

To explore the curing reaction mechanism between the BMI and BIIR in detail, 5-phr BMI was mixed with IIR, and its curing profile was generated at 180 °C for 1 h, as depicted in Figure 3(a). As shown in this figure, we observed that the curing curve of IIR with 5-phr BMI did not show any significant rise in torque due to crosslinking for a period of 1 h, even at a temperature of 180 °C. This means that BMI did not react with IIR and produced no chemical bonds between the polymer chains to enhance the rheometric torque. Figure 3(b) shows the curing curves of a 5-phr BMI–BIIR system at different temperatures, 160, 170, 180, and 190 °C, up to a reaction time of 1 h. As shown in the figure, the BMI/BIIR system showed marching modulus curing behavior with considerable reaction torque even at 160 °C, although the reaction rate was very slow. As the temperature increased, the rate of curing and the torque due to crosslinking (state of curing) gradually increased. For instance, the torque produced at 190 °C was 187% higher than that produced at 160 °C for a period of 1 h. These observations indicate

Table II. Curing Characteristics of Compounds A and B

Compound	M_H (dNm)	M_L (dNm)	ΔM ($M_H - M_L$)	T_{S2} (min)	T_{90} (min)	Curing rate index
A[a]						
160 °C	9.5	5.2	4.3	6.9	18.1	8.9
170 °C	10.0	4.7	5.3	4.4	11.5	14.1
180 °C	9.4	4.6	4.8	3.2	6.8	27.7
190 °C	8.8	4.9	3.9	2.8	6.2	30.0
B[b]						
1-phr BMI	12.3	5.0	7.3	11.9	23.5	8.6
3-phr BMI	18.3	4.5	13.8	14.3	37.8	4.3
5-phr BMI	21.4	4.1	17.3	14.2	46.4	3.1
10-phr BMI	22.4	3.3	19.1	11.6	49.7	2.6

M_H, maximum torque; M_L, minimum torque.
[a] Curing characteristics were obtained for a period of 30 min.
[b] Curing characteristics were obtained for a period of 1 h.

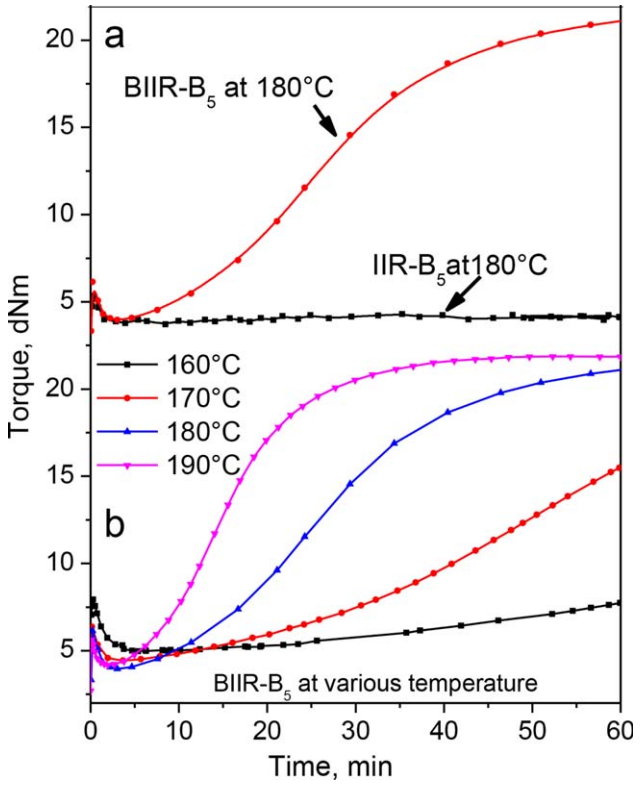

Figure 3. Curing characteristics of (a) IIR with 5-phr BMI (IIR-B_5) at 180 °C and (b) BIIR with 5-phr BMI (IIR-B_5) at various temperatures. [Color figure can be viewed in the online issue, which is available at wileyonlinelibrary.com.]

that BMI could react with BIIR and produced chemical bonds between the polymer chains. Hence, at this point, it was reasonable to believe that the allylic bromide functionality in BIIR was one of the key factors influencing the crosslinking reaction between BIIR and BMI.

It has been reported in the literature that at high temperature, bromobutyl rubber undergoes thermal dehydrohalogenation to produce the conjugated diene butyl. The evolution of such a conjugated diene via dehydrobromination highly depends on the temperature and time.[31] It is a well-known fact that a conjugated diene and a dienophile, when heated at high temperature, follow a Diels–Alder reaction.[32] Hence, in our system, it was reasonable to believe that the conjugated diene formed *in situ* as a consequence of the dehydrobromination of BIIR at the vulcanization temperature (>160 °C) could react with the diene portions of the BMI to form a cyclic adduct; this would lead to a crosslinked structure, as depicted in Scheme 1. Because IIR did not have allylic halide functionality, it could not generate a conjugated diene via dehydrohalogenation, as observed in the case of BIIR. Hence, it could not form crosslinks with bismaleimides.

Mechanical Properties of the BMI-Cured Compounds

The stress–strain behavior and corresponding tensile properties of the BMI-cured BIIR (compounds A and B) are shown in Figure 4 and Table III, respectively. Here, the test sample for the sulfur-cured compound was molded as per the respective curing time obtained from the rheometry data at 160 °C. However, because of the marching modulus curing behavior of the BIIR/BMI compounds, a molding time of 1 h was used, regardless of the concentration of BMI at a molding temperature of 180 °C. As shown in the figure, the gum vulcanizate of sulfur-cured BIIR showed the highest elongation at break and tensile strength but possessed poor low-strain modulus compared to the gum vulcanizate of BIIR and BMI. This might have been due to the flexibility of —S—S— crosslinks (especially the polysulfide linkages present in the network) and also the ability of such crosslinks to break and reform to reduce the stress concentration in the highly strained state.[33] The lower crosslinking density in the vulcanizate of the sulfur-cured BIIR might have been another reason for the higher elongation and lower stiffness or modulus.

On the contrary, the BMI-cured BIIR exhibited a lower elongation and tensile strength compared to the sulfur-crosslinked one but possessed a higher modulus and hardness. For instance, the modulus at a 50% elongation of the 1-phr BMI-cured gum vulcanizate was 16% higher than that of the sulfur-cured one and rose further to 90% by crosslinking with 10-phr BMI. Likewise, the hardness of 1-phr BMI-cured compound was 37% higher

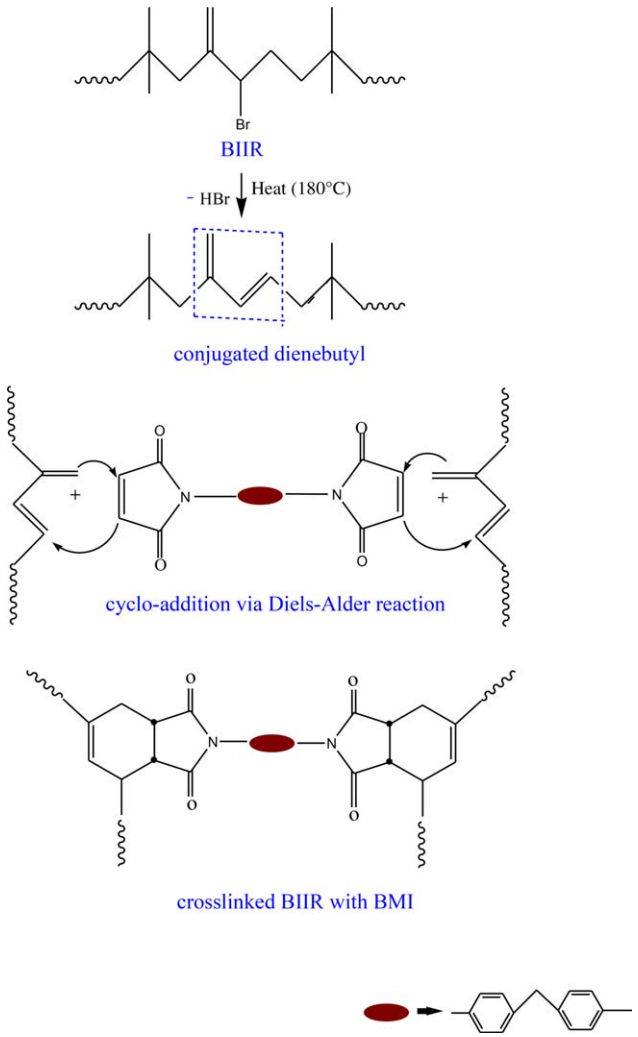

Scheme 1. Proposed crosslinking reaction mechanism between BMI and BIIR at high temperatures. [Color figure can be viewed in the online issue, which is available at wileyonlinelibrary.com.]

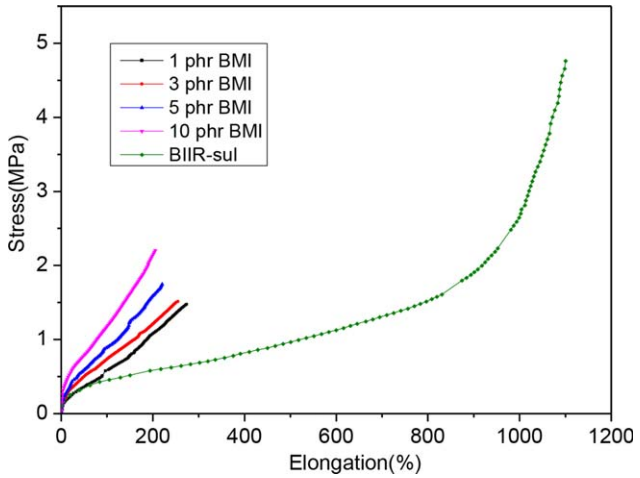

Figure 4. Stress–strain behaviors of sulfur-cured BIIR and BIIR cured with different concentrations of BMI. [Color figure can be viewed in the online issue, which is available at wileyonlinelibrary.com.]

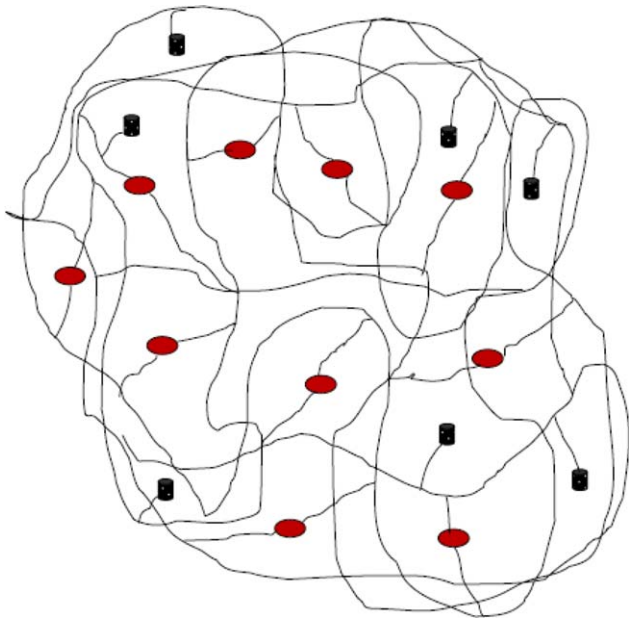

Figure 5. BMI units incorporated into the BIIR networks as crosslinkers (red) and danglers (black). [Color figure can be viewed in the online issue, which is available at wileyonlinelibrary.com.]

than that of the sulfur-cured one and rose further to 62% with 10-phr BMI. This improvement in the mechanical properties, especially the modulus and hardness of the BMI-cured gum vulcanizate, was very similar to the effect produced by a reinforcing filler of high modulus. It has been reported that when diene rubbers are heated with bismaleimide, some BMI units can graft into the elastomeric network in addition to the crosslinked units,[34,35] as represented in Figure 5. The grafted BMI units may act as reinforcing filler in addition to their role as a crosslinking agent; this ultimately leads to the formation of a tightly crosslinked network structure with a higher stiffness. This tight network structure in the vulcanizate of BIIR and BMI strongly resisted tensile deformation, particularly at a lower strain. As a result, it showed a higher modulus than the sulfur-crosslinked BIIR. However, because of the stiff network structure in the vulcanizate of BIIR and BMI, there was a high stress concentration in the matrix because of its inability to dissipate the strain energy. As a result, their vulcanizates underwent breakage at a relatively low elongation.

Effects of DCP and ZnO on the Curing Efficiency of BMI/BIIR

For a fast production cycle in the manufacturing process of a rubber article, it is always recommended that one complete the curing cycle as fast as possible and provide good scorch safety. We observed that the curing of BIIR with BMI alone was very slow even at high temperature, although it offered a high state of curing (higher ΔM) compared to the sulfur-accelerated curing system. Hence, to achieve a curing plateau with a maximum torque in the lowest possible time at the lowest possible vulcanization temperature for the BMI curing of BIIR, we used DCP and ZnO to activate the crosslinking reaction between BIIR and BMI.

Figure 6(a) presents the curing profiles of pristine BIIR with 2.5-phr ZnO alone (BIIR-$Z_{2.5}$), 5-phr BMI alone (BIIR-B_5), and 5-phr BMI in conjunction with 2.5- and 5-phr ZnO (BIIR-$B_5Z_{2.5}$ and BIIR-B_5Z_5, respectively) at 160 °C for 1 h. Similarly, Figure 6(b) represent the curing profiles of BIIR with 0.25-phr DCP alone (BIIR-$D_{0.25}$), 5-phr BMI alone (BIIR-B_5), and 5-phr BMI in conjunction with different concentrations of DCP (0.25–3 phr) at 160 °C for 30 min. Their curing characteristics are summarized in Table IV. As shown in Figure 6(a), ZnO alone can crosslink BIIR at a relatively faster rate compared to the crosslinking between BIIR and BMI. Moreover, the curing curve of BIIR with ZnO showed a plateau region beyond 30 min with excellent overcure stability up to 1 h. The ability of ZnO to produce a stable carbon–carbon crosslink in the vulcanizate might have been the reason behind the overcure reversion stability. It was very interesting that the presence of ZnO dramatically accelerated the curing of BIIR with BMI and exhibited

Table III. Mechanical Properties of BIIR with Different BMI Contents

BMI content (phr)	Tensile strength (MPa)	50% modulus (MPa)	100% modulus (MPa)	Elongation at break (%)	Hardness (Shore A)
1	1.5 ± 0.07	0.42 ± 0.03	0.67 ± 0.05	252 ± 10	31 ± 1
3	1.5 ± 0.03	0.50 ± 0.04	0.72 ± 0.05	252 ± 26	40 ± 1
5	1.8 ± 0.09	0.56 ± 0.04	0.82 ± 0.06	244 ± 39	43 ± 2
10	2.3 ± 0.12	0.69 ± 0.05	1.05 ± 0.06	222 ± 20	47 ± 1

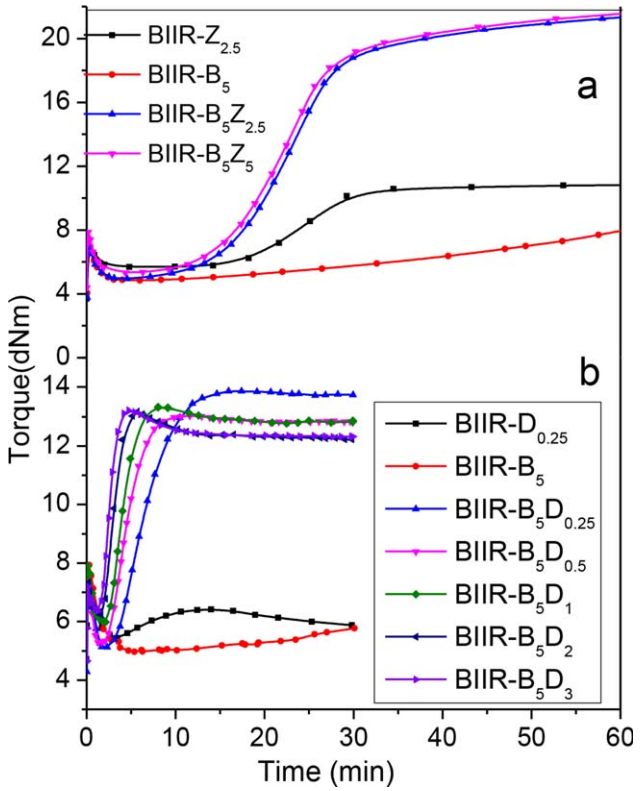

Figure 6. Curing characteristics of BIIR with 5-phr BMI at 160 °C and with different contents of (a) ZnO and (b) DCP. [Color figure can be viewed in the online issue, which is available at wileyonlinelibrary.com.]

a higher state of curing. For instance, the addition of 2.5-phr ZnO along with BMI enhanced the crosslinking torque to about 90% compared to ZnO-only curing and to 230% compared to BMI-only curing at a reaction time of 30 min. Moreover, the curing curves of BIIR with BMI/ZnO exhibited a curing plateau beyond 40 min of curing with excellent reversion resistance. Increasing the concentration of ZnO beyond 2.5 phr did not produce any significant improvement in the crosslinking torque or reduce the curing time. In the literature, it has been well established that heating halogenated butyl rubber with ZnO produces a conjugated diene in the polymer chain via dehydrohalogenation with the formation of zinc dihalide (ZnX_2).[9] Hence, the faster curing dynamics with a higher level of curing observed in the crosslinking of BIIR with BMI in the presence of ZnO was ascribed to the effect of two parallel reactions. One might have been the Diels–Alder reaction between the conjugated dienebutyl generated *in situ* with the dienophile part of the bismaleimide, as depicted in Scheme 1. The other one was the ZnO vulcanization initiated by $ZnBr_2$, formed *in situ* as postulated by Baldwin *et al.* and supported by Kuntz *et al.*[36] and Vukov.[9,37] The rate and state of curing of BIIR-B_5 at 190 °C were more or less the same as the curing dynamics observed for BIIR and BMI in the presence of ZnO at 160 °C. Hence, we believe that the presence of ZnO accelerated the conjugated dienebutyl formation and favored the Diels–Alder reaction with BMI to take place at a lower temperature while acting itself as a crosslinking agent for BIIR.

As shown in Figure 6(b), BIIR exhibited a marginal reaction torque for a while upon heating with DCP as a sole curing agent and then underwent reversion after a reaction time of 15 min. This was due to the inherent instability of the butyl polymers upon reaction with peroxide, as has been reported well in the literature.[23] On the other hand, the curing curve of BIIR-B_5 did not produce any significant rise in torque, even up to a reaction time of 30 min. However, the curing profile of BIIR with BMI in conjunction with 0.25-phr DCP (BIIR-$B_5D_{0.25}$) showed a dramatic rise in torque with a curing plateau within 15 min and exhibited good overcure stability (no reversion tendency) up to a reaction time of 30 min. As the concentration of peroxide increased from 0.25 to 3 phr, the curing time gradually decreased. However, ΔM and the scorch safety decreased as the peroxide concentration increased. As a result, it is always recommended that one use the optimum concentration of DCP to maintain the best overall performance. On the basis of the curing data as given in Table IV, we optimized the BMI/DCP

Table IV. Curing Characteristics of Compounds C and D

Compound	M_H (dNm)	M_L (dNm)	ΔM ($M_H - M_L$)	T_{S2} (min)	T_{90} (min)	Curing rate index
C[a]						
2.5-phr ZnO	22.4	4.9	17.5	15.9	46.8	3.2
5.0-phr ZnO	22.9	5.3	17.6	15.5	51.0	2.8
D[b]						
0.25-phr DCP	13.9	5.1	8.8	4.7	10.5	17.5
0.5-phr DCP	13.0	5.3	7.7	3.5	7.0	28.7
1.0-phr DCP	13.3	6.0	7.3	3.4	5.7	42.6
2.0-phr DCP	13.2	6.2	7.0	2.6	4.2	61.7
3.0-phr DCP	13.2	6.4	6.8	2.2	3.5	76.9
BIIR + 2.5-phr ZnO[a]	11.2	5.7	5.5	23.0	34.9	8.4
BIIR + 0.25-phr DCP[b]	6.5	5.5	1.0	—	—	—

M_H, maximum torque; M_L, minimum torque.
[a] Curing characteristics were obtained for a period of 1 h.
[b] Curing characteristics were obtained for a period of 30 min.

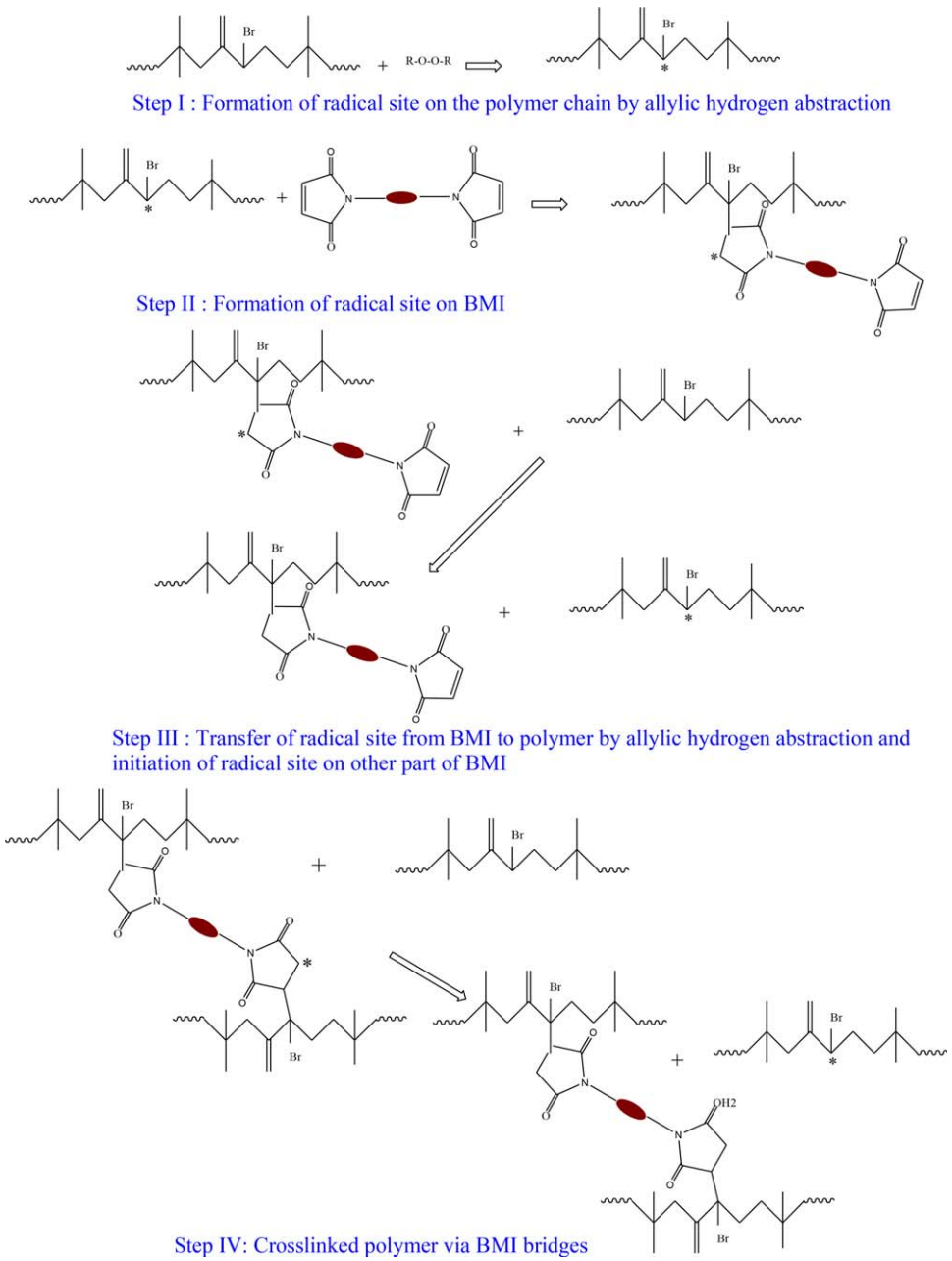

Scheme 2. Proposed crosslinking reaction mechanism between BMI and BIIR in the presence of DCP. [Color figure can be viewed in the online issue, which is available at wileyonlinelibrary.com.]

ratio as 1:0.05 to maintain a balance of curing rate, scorch safety, maximum rheometric torque, and reversion resistance at 160 °C.

Proposed Crosslinking Mechanism between BIIR and BMI in the Presence of DCP

Unlike the crosslinking mechanism observed in BIIR/BMI or BIIR/BMI in the presence of ZnO, the crosslinking reaction between BIIR and BMI in the presence of DCP followed a radical initiation reaction through hydrogen atom abstraction, as depicted in Scheme 2. Upon heating BIIR and BMI in the presence of peroxide, the peroxide decomposed and abstracted a hydrogen atom from the allylic bromide functionality to form a radical site on the polymer chain (step I). Once the radical was formed, the BMI was added quickly to it. By doing so, a new radical site was generated on the BMI (step II). The radical on the BMI again abstracted allylic hydrogen from another polymer chain, and this resulted in a new polymer radical (step III). At this stage, the other site of maleimide units of BMI repeated the reaction observed in steps II and III to form bismaleimide bridges (crosslinks) between the polymer chains, as depicted in step IV.

Effect of the Temperature on the Curing Characteristics

The vulcanization characteristics of gum BIIR with the sulfur-curing system (BIIR-sul), 5-phr BMI alone (BIIR-B_5), BMI in conjunction with an optimum level of DCP (BIIR-$B_5D_{0.25}$),

Table V. Curing Characteristics of BIIR with the Sulfur-Curing System and the BMI-Curing System

Compound	Temperature	ΔM	T_{S2} (min)	T_{90} (min)	Curing rate index
BIIR-sul[a]	160 °C	4.3	6.9	18.1	8.9
	170 °C	5.3	4.4	11.5	14.1
	180 °C	4.7	3.2	6.8	27.7
	190 °C	3.9	2.8	6.2	30.0
BIIR-B_5[b]	160 °C	2.8	50.0	56.5	No effective curing
	170 °C	11.1	23.4	55.9	3.1
	180 °C	17.3	14.2	46.4	3.1
	190 °C	17.7	7.9	28.0	5.0
BIIR-$B_5Z_{2.5}$[b]	160 °C	17.5	15.9	46.8	3.2
	170 °C	18.8	8.5	31.2	4.3
	180 °C	19.0	5.0	22.4	5.7
	190 °C	19.3	3.1	11.7	11.6
BIIR-$B_5D_{0.25}$[a]	160 °C	8.7	4.7	10.5	17.4
	170 °C	7.3	2.9	4.8	51.5
	180 °C	5.6	2.2	3.2	102.0
	190 °C	5.2	1.5	2.0	185.2
BIIR-$B_5Z_{2.5}$ $D_{0.25}$[a]	160 °C	10.4	5.1	14.8	10.4
	170 °C	8.7	3.0	6.7	27.0
	180 °C	7.5	1.9	4.0	47.8
	190 °C	6.3	1.6	2.6	94.3

[a] Curing characteristics were obtained for a period of 30 min.
[b] Curing characteristics were obtained for a period of 1 h.

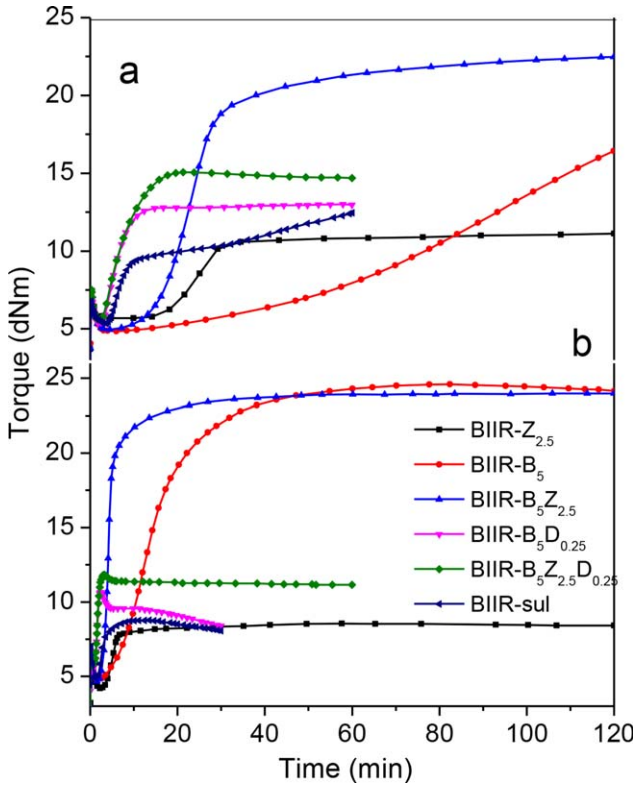

Figure 7. Curing characteristics of the vulcanizates with different reaction times at (a) 160 and (b) 190 °C. [Color figure can be viewed in the online issue, which is available at wileyonlinelibrary.com.]

BMI in conjunction with optimum level of ZnO (BIIR-$B_5Z_{2.5}$), and BMI in conjunction with a combination of DCP and ZnO (BIIR-$B_5D_{0.25}Z_{2.5}$) at four different temperatures, 160, 170, 180, and 190 °C, is tabulated in Table V. Representative curing curves of the same compounds at 160 and 190 °C are depicted in Figure 7(a,b).

The decrease in curing time (faster curing rate) with increasing temperature is a commonly observed phenomenon in any vulcanization process. This also remained true in the curing characteristics of the compound tabulated in Table V. In addition to this, as shown in the table, sulfur curing did not reduce the state of curing (ΔM) significantly with increasing temperature, but it exhibit a severe overcure reversion at elevated temperature (>180 °C). On the other hand, the vulcanization of BIIR-$B_5D_{0.25}$ showed a gradual decrease in ΔM with poor overcure reversion stability with increasing temperature. For instance, although the sulfur curing of BIIR reduced ΔM to about 10% at 190 °C, a 40% reduction in ΔM was observed during the curing of BIIR-$B_5D_{0.25}$ at the same temperature. The reversion in the cured rubber compound mainly occurred because of the loss of crosslinking network upon thermal aging. The reversion process ultimately led to a weakening of the mechanical performance of the rubber compound. The overcure reversion observed in BIIR-sul at high temperature was attributed to the breakdown of polysulfide bonds generated in the vulcanizate. We pointed out in the Mechanical Properties section that the optimum ratio of BMI to DCP was 1:0.05 at 160 °C for a balanced curing rate, curing state, and overcure reversion resistance

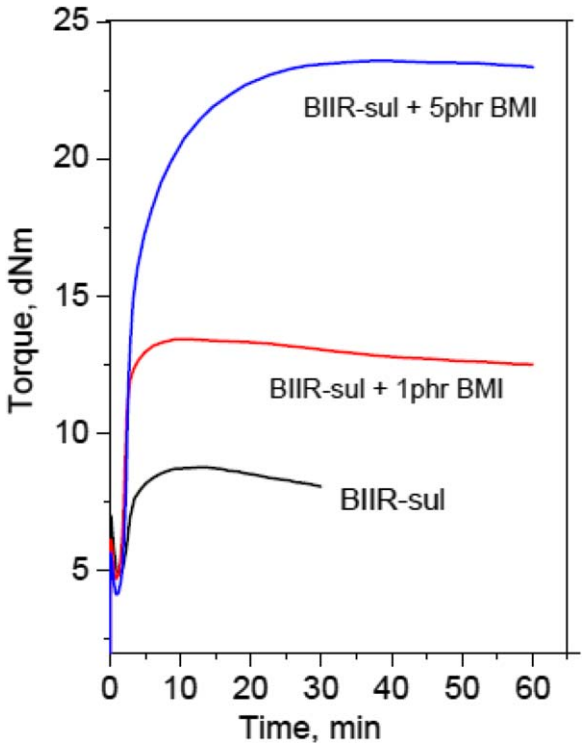

Figure 8. Curing characteristics of BIIR-sul with 1-phr BMI and 5-phr BMI at 190 °C. [Color figure can be viewed in the online issue, which is available at wileyonlinelibrary.com.]

of the compound BIIR-$B_5D_{0.25}$. Hence, the reason for the severe overcure reversion observed in BIIR-$B_5D_{0.25}$ at high temperature (>160 °C) might have been the degradation of the butyl polymer by the action of excess peroxide radical generated at high temperature.

Also, as shown in Table V, the state of curing (ΔM) for the compound BIIR-$B_5D_{0.25}Z_{2.5}$ than that of BIIR-$B_5D_{0.25}$ at all temperatures from 160 to 190 °C. Moreover, the former one possessed better overcure reversion stability than the latter even at 190 °C for a reaction time up to 1 h. The higher state of curing with improved overcure reversion observed in BIIR-$B_5D_{0.25}Z_{2.5}$ might have been due to the presence of more crosslinks in the vulcanizate because of the possibilities of two reactions: one as shown in Scheme 1, accelerated by ZnO, and the other one as shown in Scheme 2, accelerated by DCP. As a result of this, the vulcanizate of BIIR-$B_5D_{0.25}Z_{2.5}$ became tighter with high crosslinking density and, hence, possessed good overcure reversion stability at high temperature compared to BIIR-$B_5D_{0.25}$. However, when analyzing the curing behavior of BIIR-$B_5D_{0.25}Z_{2.5}$ itself under different temperatures, we observed that the state of curing decreased as the temperature increased. For instance, the ΔM value produced by this compound at 190 °C was 40% less than that produced at 160 °C. This was attributed to the fact that at lower temperature (160 °C), the torque was partly contributed by the crosslinks formed due to the reaction shown in Scheme 1 and partly due to reaction shown in Scheme 2. As the temperature increased, the radical reaction present in Scheme 2 was predominant because of its high rate of vulcanization. As a result, the compound viscosity may have increased within few seconds for the reaction shown in Scheme 1 to take place in a significant level. Nevertheless, the possibility of such coreactions could not be discarded completely even at high temperatures. The higher ΔM values possessed by BIIR-$B_5D_{0.25}Z_{2.5}$ at all of the vulcanization temperatures compared to BIIR-$B_5D_{0.25}$ strongly support this possibility.

Unlike in the case of BIIR-$B_5D_{0.25}$ or BIIR-$B_5D_{0.25}Z_{2.5}$, the noteworthy feature in the vulcanization of BIIR-$B_5Z_{2.5}$ was that it exhibited a high state of curing with increasing temperature. For instance, the ΔM value produced by BIIR-$B_5Z_{2.5}$ was 207% higher than that produced by BIIR-$B_5Z_{2.5}D_{0.25}$ at 190 °C, even though both compounds contained the same amount of ZnO. In addition, it showed good processing safety (scorch safety) with excellent overcure reversion resistance even at 190 °C for 2 h. The discrepancy in the ΔM values of these two compounds during vulcanization could be explained on the basis of their vulcanization chemistry. As explained previously, the vulcanization of BIIR-$B_5D_{0.25}Z_{2.5}$ predominantly followed the chemical reaction mechanism depicted in Scheme 2. On the contrary, in BIIR-$B_5Z_{2.5}$, there was an equal possibility of ZnO-only crosslinking and BMI-alone crosslinking. As reported by Vukov,[9] the ZnO could crosslink BIIR via conjugated diene butyl as the intermediate. This conjugated diene butyl generated *in situ* was responsible for the BMI crosslinking of BIIR, as represented in Scheme 1. As shown in the scheme and as was expected, the crosslinking efficiency (curing rate) of ZnO alone with BIIR increased from 160 to 190 °C. However, even though there was no reversion, ΔM decreased by about 20% as the temperature increased to 190 °C. This might have been due to the fact that at high temperature, more conjugated diene butyl was generated via dehydrobromination. This may have reduced the availability of bromine atoms for the formation of carbon–carbon crosslinks by the action of zinc halide but could have increased the number of BMI bridges between the polymer chains via the reaction shown in Scheme 1 because of the availability of more conjugated diene butyl at high temperature. The higher torque observed during the crosslinking of BIIR with a combination of BMI and ZnO at 190 °C strongly supported this statement.

The reversion resistance of BMI was also tested during sulfur vulcanization. Depicted in Figure 8 are the curing characteristics of BIIR-sul with 1-phr BMI and also with 5-phr BMI at 190 °C. As shown in the figure, the sulfur-cured BIIR showed a severe reversion after 10 min of curing. However, its reversion resistance was significantly improved with the use of BMI at the same temperature. For instance, the vulcanization of BIIR-sul along with 5-phr BMI was found to be stable even up to 1 h. In addition, it offered tremendous improvement in the state of curing (higher ΔM) by acting as a crosslinker itself. For instance, ΔM increased to 125 and 400% with the use of 1- and 5-phr BMI, respectively.

DSC Analysis

To further confirm the proposed crosslinking mechanism, isothermal DSC analysis was also performed under different temperature conditions. Figure 9(a,b) shows the isothermal DSC curves of the compounds BIIR-sul, BIIR-B_5, BIIR-$B_5D_{0.25}$, BIIR-$B_5Z_{2.5}$, and BIIR-$B_5D_{0.25}Z_{2.5}$ at two extreme temperatures of 160

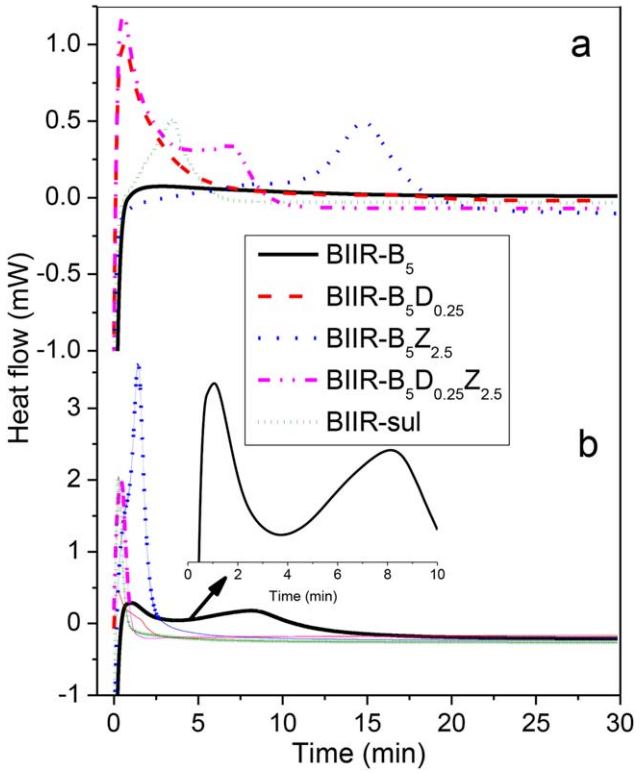

Figure 9. Isothermal DSC curves of the vulcanizates at (a) 160 and (b) 190 °C for 30 min. [Color figure can be viewed in the online issue, which is available at wileyonlinelibrary.com.]

and 190 °C, respectively. We observed that the reaction between BIIR and BMI (BIIR-B_5) at 160 °C did not produce any exothermic peak responsible for the crosslinking up to a reaction time of 30 min. However, when the temperature was increased to 190 °C, BIIR-B_5 showed two mild exothermic peaks at 1 and 8 min. The peak at 1 min might have been due to the grafting of BMI units onto the polymer chains or to the Alder–ene reaction between BMI and the isoprene unit in BIIR,[35] and the peak at 8 min was probably due to the Diels–Alder reaction depicted in Scheme 1. The activation of BMI with 0.25-phr DCP, 2.5-phr ZnO, or a combination of 0.25-phr DCP and 2.5-phr ZnO generated distinct exothermic peaks, with peak maxima appearing at 15 min for BIIR-$B_5Z_{2.5}$, 33 s for BIIR-$B_5D_{0.25}$, and at 36 s for BIIR-$B_5D_{0.25}Z_{2.5}$ at 160 °C. When the temperature was increased, the curing exotherms for all of the compounds shifted to shorter timescales.

However, it should be emphasized here that the rate of curing for the compound BIIR-$B_5Z_{2.5}$ was significantly accelerated when the temperature was increased; this could be clearly visualized from its isothermal DSC trace, depicted in Figure 10(a). The curing exothermic peak appearing at 15 min at 160 °C was shifted to 1.45 min along with much higher enthalpy of curing at 190 °C. This was in good agreement with the high state of curing (higher ΔM) of this compound observed in the rheometric studies with increasing temperature. This strongly supported the fact that ZnO accelerated the formation of conjugated dienebutyl at higher temperatures and quickened the Diels–Alder reaction to form crosslinks. The exothermic peaks of other compounds appeared at more or less the same positions; this indicated that these compounds could be effectively crosslinked at a relatively lower temperature (160 or 170 °C). The DSC trace of the compound BIIR-$B_5D_{0.25}Z_{2.5}$, shown in Figure 10(b), explained why the level of curing (ΔM) decreased with increasing temperature. There were two exothermic peaks during the crosslinking reaction at 160 °C: a major one at 35 s and another one at 7 min. The peak at 35 s was responsible for the crosslinking of BIIR by the action of BMI and DCP, and the peak at 7 min was probably due to the crosslinking of BIIR by the action of BMI and ZnO via the Diels–Alder reaction. Interestingly, the intensity of the second peak became feeble, and its position shifted to the lower end of the timescale with increasing temperature. This peak completely disappeared at 190 °C and left only one peak, which was due to the crosslinking of BIIR with BMI and DCP. This indicated that when BIIR was heated at high temperature (190 °C) with BMI in conjunction with ZnO and DCP, the crosslinking reaction mainly followed Scheme 2. However, when the same compound was heated at a relatively lower temperature (160 °C), it exhibited higher values of ΔM; this was probably due to the possibilities of both crosslinking reactions, as depicted in Schemes 1 and 2. This could have been one of the primary reasons why the state of curing in this compound decreased with increasing temperature.

Thermal Stability of the Vulcanizates

There is a continuing need for elastomers capable of withstanding high temperatures. The crosslinking agent, which can generate

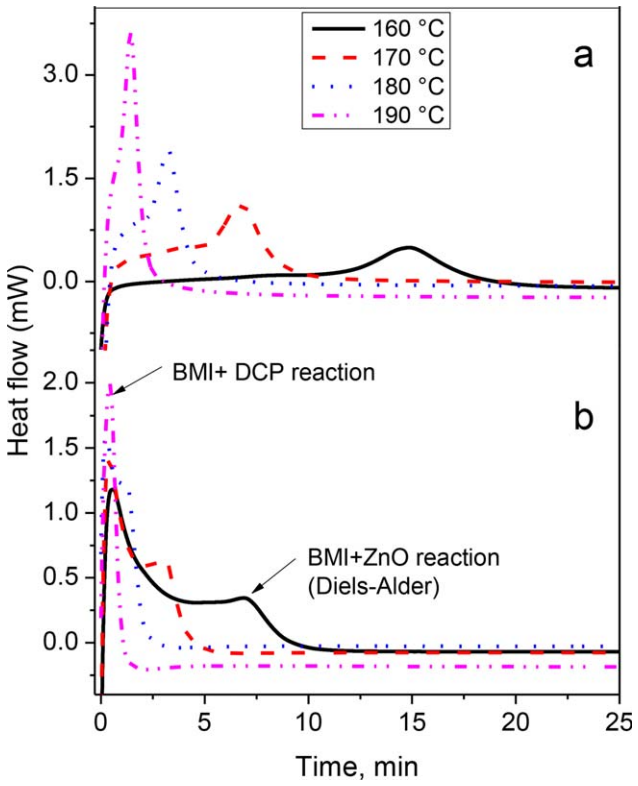

Figure 10. Isothermal DSC curves of (a) BIIR-$B_5Z_{2.5}$ and (b) BIIR-$B_5D_{0.25}Z_{2.5}$ at different temperatures. [Color figure can be viewed in the online issue, which is available at wileyonlinelibrary.com.]

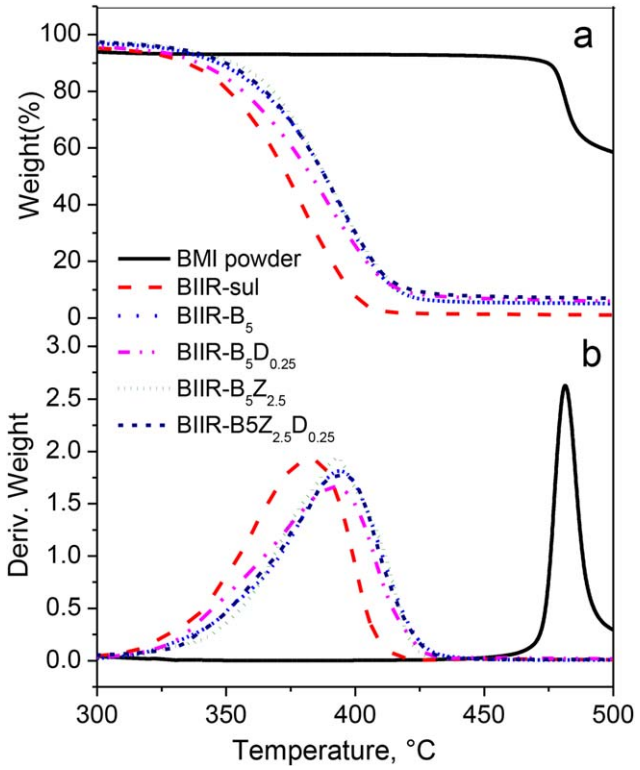

Figure 11. (a) TGA thermograms and (b) their derivatives for the pure BMI powder and its vulcanizates with BIIR. [Color figure can be viewed in the online issue, which is available at wileyonlinelibrary.com.]

stable crosslinks between the polymer chains, has a major role for increasing the thermal stability of the elastomeric materials. To understand the influence of different curing systems on the thermal stability of the vulcanizates, TGA was performed. Figure 11 shows the TGA thermograms and their derivatives of the neat BMI. Because of its inherent thermal stability, the neat BMI showed the onset of thermal degradation at a very high temperature (480 °C). The TGA and derivative thermograms of the BMI-cured BIIR and sulfur-cured BIIR are also included in the same figure for comparison purposes. In contrast to the sulfur-cured BIIR, the onset and maximum degradation temperatures were shifted to a higher temperature regime for the all of the vulcanizates of BIIR containing BMI. This strongly indicated that the BMI-cured BIIR compounds were thermally more stable than the sulfur-cured BIIR. Sulfur-cured BIIRs generally possess either carbon–sulfur (—C—S—) or sulfur–sulfur (—S—S—) crosslinks in their network structure. All of these bonds are thermally less stable than carbon–carbon (—C—C—) bonds. On the other hand, the vulcanizates BIIR-B_5, BIIR-$B_5Z_{2.5}$, BIIR-$B_5D_{0.25}$, and BIIR-$B_5D_{0.25}Z_{2.5}$ may comprise a combination of BMI bridges between the polymer chains, loosely embedded BMI units due to grafting, and certain direct carbon–carbon (—C—C—) linkages between polymer chains by the action of ZnO or DCP. All of these crosslinks are very strong and produce vulcanizates of tight network structure with a high crosslinking density. As a result, their vulcanizates shows enhanced thermal stability. The inherent high-temperature stability of the bismaleimide resin might also be one of the reasons for the improved thermal stability.

Table VI. Crosslinking Densities Estimated with the Swelling Method and the Mooney–Rivlin Method

Vulcanizate	Swelling method: n (mol/cc)	Mooney–Rivlin method	
		C_1 (MPa)	n_{phy} (mol/cc)
BIIR-sul	7.22×10^{-5}	0.055	2.26×10^{-5}
BIIR-$B_5D_{0.25}$	1.46×10^{-4}	0.133	5.36×10^{-5}
BIIR-$B_5Z_{2.5}$	3.05×10^{-4}	0.413	1.67×10^{-4}
BIIR-$B_5D_{0.25}Z_{2.5}$	1.67×10^{-4}	0.255	1.03×10^{-4}

Crosslinking Density and Mechanical Properties of the Vulcanizate

The crosslinking densities measured via equilibrium swelling testing for the selected compounds are listed in Table VI. As shown, the crosslinking densities of the vulcanizates followed the order BIIR-sul < BIIR-$B_5D_{0.25}$ < BIIR-$B_5D_{0.25}Z_{2.5}$ < BIIR-$B_5Z_{2.5}$. This trend was in line with the ΔM values (an indirect indication of the crosslinking density) of these compounds obtained from the rheometry data. The highest crosslinking density exhibited by the compound BIIR-B_5-$Z_{2.5}$ was attributed to the bismaleimide crosslinks between the polymer chains via the Diels–Alder reaction and the carbon–carbon crosslinks

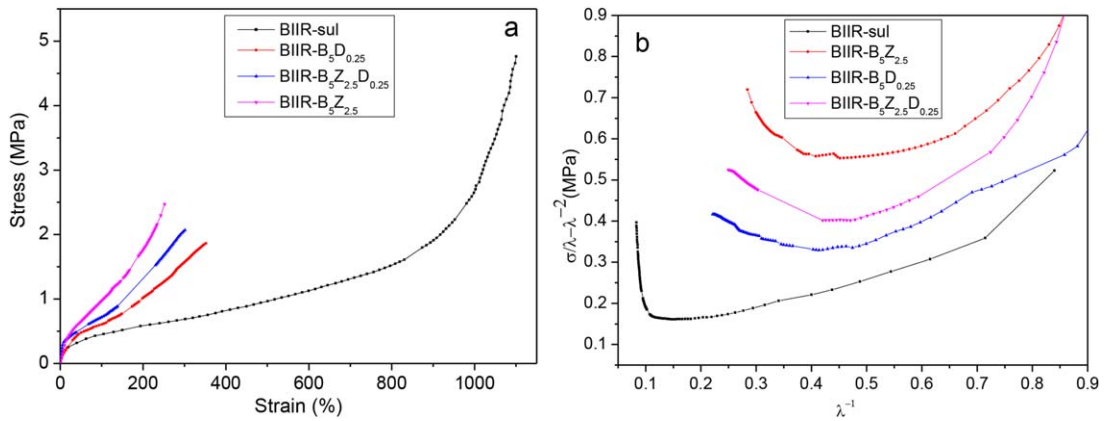

Figure 12. (a) Stress–strain curves and (b) corresponding Mooney–Rivlin plots of various vulcanizates. [Color figure can be viewed in the online issue, which is available at wileyonlinelibrary.com.]

Table VII. Mechanical Properties of the Vulcanizates

Compounds	Tensile strength (MPa)	50% modulus (MPa)	100% modulus (MPa)	Elongation at break (%)	Hardness (Shore A)
BIIR-sul	4.5 ± 0.30	0.36 ± 0.04	0.46 ± 0.02	950 ± 74	30 ± 1
BIIR-$B_5Z_{2.5}$	2.4 ± 0.20	0.65 ± 0.06	0.99 ± 0.06	238 ± 17	45 ± 1
BIIR-$B_5D_{0.25}$	1.8 ± 0.10	0.44 ± 0.04	0.62 ± 0.03	351 ± 15	36 ± 1
BIIR-$B_5Z_{2.5}D_{0.25}$	2.0 ± 0.10	0.51 ± 0.02	0.70 ± 0.03	287 ± 11	40 ± 1

generated by the action of ZnO. The stress–strain curves of the gum vulcanizates were used to evaluate the crosslinking density via the Mooney–Rivlin equation. The stress–strain behavior and the corresponding reduced stress versus 1/λ (Mooney–Rivlin plot) of the aforementioned compounds are represented in Figure 12(a,b). The reduced stress and the C_1 values of all of the vulcanizate of BIIR involving BMI crosslinks were higher compared to the sulfur-crosslinked one. Moreover, reductions in the reduced stress were observed in all of the BMI-cured vulcanizates in the low deformation region, like the Payne effect.[27] This substantiated BMI as an effective material for curing BIIR and for offering some fillerlike reinforcement to the matrix, possibly because of the grafting of some of the BMI units into the elastomeric network, as depicted in Figure 5. Although there were some discrepancies in the values of crosslinking densities determined by the equilibrium swelling test and the Mooney–Rivlin theory, the values obtained for all of the compounds from each of these methods were in good agreement with their state of curing (ΔM values) obtained from the rheometer study. However, the values obtained for all of the compounds from the Mooney–Rivlin equation were lower than those obtained from the equilibrium swelling method by the Flory–Rehner equation. Particularly for the compound: BIIR-$B_5D_{0.25}$, the value showed a large deviation by a factor of 10. These deviations may have been due to the fact that the Mooney–Rivlin equation is based on the stress–strain method, where the polymer network is subjected to tensile deformation. It is well known that the deformation behavior of a crosslinked polymer network highly depends on the type of crosslinks, the magnitude of crosslinks, and also the flexibility of the crosslinks in the network. Unlike the sulfur-cured BIIR, the compounds BIIR-$B_5Z_{2.5}$, BIIR-$B_5D_{0.25}$, and BIIR-$B_5Z_{2.5}D_{0.25}$ may have been composed of a combination of BMI bridges between the polymer chains, loosely embedded BMI units due to grafting, and short carbon–carbon (—C—C—) linkages due to crosslinking by the action of ZnO. As a result of the mixed crosslinks in these vulcanizates, their deformation behavior may have been different; this was naturally reflected in their crosslinking density values. There is no such deformation (stretching) of the polymer chain involved in determining the crosslinking density by the Flory–Rehner equation. Because it is based on the swelling method, the tightness of the network matters.

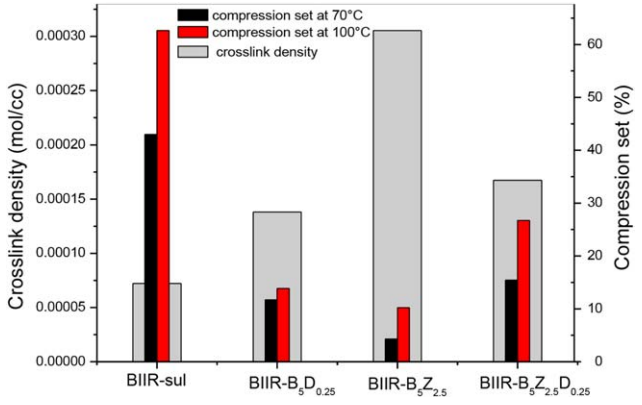

Figure 13. Crosslinking densities of the vulcanizates and their compression values measured at 70 and 100 °C. [Color figure can be viewed in the online issue, which is available at wileyonlinelibrary.com.]

The mechanical properties of the aforementioned vulcanizate are tabulated in Table VII. As shown, the sulfur-cured BIIR showed the highest elongation and ultimate tensile strength. This might have been due to the flexibility of the sulfur–sulfur crosslinks and its low crosslinking density. The elongation at break of all of the vulcanizates possessing BMI bridges drastically decreased to about 70% compared to the sulfur-cured BIIR. However, the low-strain modulus (50% modulus) and hardness showed higher values than the corresponding sulfur-cured one. This was because in the BMI-cured vulcanizate, the crosslinks involved an aromatic ring structure. These types of crosslinks make the network stiff and less flexible and naturally enhance the modulus and hardness. Because of the same reasons, the BMI-cured vulcanizate exhibited much lower compression set values than the sulfur-cured BIIR vulcanizate at both 70 and at 100 °C, as shown in Figure 13. When we analyzed the set values of these vulcanizates in the light of their ΔM value and the crosslinking density, we observed that as the crosslinking density (ΔM) increased, the compression set decreased.

CONCLUSIONS

For the development of thermally stable bromobutyl rubber with a high crosslinking density, BMI was newly applied to crosslink BIIR. On the basis of the rheometric analyses, we found that BMI alone could be used as a crosslinking agent for BIIR, and the resulting vulcanizate provided a high crosslinking density with an excellent overcure reversion stability compared to its corresponding sulfur-cured system. Additionally, we realized that the conjugated dienebutyl function generated by dehydrobromination seemed to be the precursor for the crosslinking reaction of BIIR with BMI, similar to the Diels–Alder reaction. Because the BMI-based reaction was relatively slow even at a high temperature, either ZnO or DCP was introduced as a crosslinking reaction accelerator. The ZnO crosslinking accelerator dramatically increased the curing rate of the BMI-based

system, particularly at high temperature (190 °C), with an excellent scorch safety. The BMI-based BIIR vulcanizate in the presence of ZnO exhibited the highest crosslinking density with superior set properties at elevated temperature. The faster curing rate in the presence of ZnO originated from the increased speed and quantity of conjugated dienebutyl formation between BIIR and BMI. DCP also worked as a crosslinking reaction accelerator in the BMI-based system. On the basis of the considerations of the curing rate, scorch safety, maximum rheometric torque, and reversion resistance at 160 °C, the DCP content was optimized to be BMI/DCP = 1:0.05. We successfully demonstrated that the BMI-cured BIIR exhibited a higher crosslinking density with superior low compression set properties at elevated temperatures and excellent thermal stability compared to conventional sulfur-cured BIIR.

REFERENCES

1. Fusco, J. V.; Hous, P. In Rubber Technology, 3rd ed.; Morton, M., Ed.; Van Nostrand Reinhold: New York, **1987**; p 290.
2. Newman, N. F.; Fusco, J. V. In Handbook of Elastomers, 2nd ed.; Bhomick, A. K., Stephans, H. L., Eds.; Marcel Decker: New York, **2001**; p 877.
3. Gan, L. M.; Chew, C. H. *J. Appl. Polym. Sci.* **1979**, *24*, 371.
4. Yanbing, W.; Chenguang, Z.; Hao, Y.; Zhixiong, H. *J. Macromol. Sci. Phys.* **2014**, *53*, 813.
5. Vukov, R. *Rubber Chem. Technol.* **1984**, *57*, 275.
6. Chu, C. Y.; Watson, K. N.; Vukov, R. *Rubber Chem. Technol.* **1987**, *60*, 636.
7. Parent, J. S.; Thom, D. J.; White, G.; Whitney, R. A.; Hopkins, W. J. *J. Polym. Sci. Part A: Polym. Chem.* **2001**, *39*, 2019.
8. Malmberg, S. M.; Parent, J. S.; Pratt, D. A.; Whitney, R. A. *Macromolecules* **2010**, *43*, 8456.
9. Vukov, R. *Rubber Chem. Technol.* **1984**, *57*, 284.
10. Shinzo, Y.; Kazutoshi, K.; Yuko, I.; Shinzo, K. *J. Polym. Sci. Part A: Polym. Chem.* **1993**, *31*, 2437.
11. Yuko, I.; Kazutoshi, K.; Kanji, K.; Shinzo, K. *J. Polym. Sci. Part B: Polym. Phys.* **1995**, *33*, 387.
12. Yuko, I.; Yuka, N.; Kanji, K.; Shinzo, K. *J. Polym. Sci. Part A: Polym. Chem.* **1995**, *33*, 2657.
13. Parent, J. S.; White, G. D.; Whitney, R. A. *Macromolecules* **2002**, *35*, 3374.
14. Gullien-Castellanos, S. A.; Parent, J. S.; Whitney, R. A. *Macromolecules* **2006**, *39*,2514.
15. Gullien-Castellanos, S. A.; Parent, J. S.; Whitney, R. A. *J. Polym. Sci. Part A: Polym. Chem.* **2006**, *44*, 983.
16. Parent, J. S.; White, G. D.; Thom, D. J.; Whitney, R. A.; Hopkins, W. *J. Polym. Sci. Part A: Polym. Chem.* **2003**, *41*, 1915.
17. Parent, J. S.; Penciu, A.; Guillen-Castellanos, S. A.; Liskova, A.; Whitney, R. A. *Macromolecules* **2004**, *37*, 7477.
18. Amit, D.; Aladdin, S.; Frank, B.; Marcus, S.; Debdipta, B.; Sven, W.; Klaus, W. S.; Brigitte, V.; Gert, H. *ACS Appl. Mater. Interfaces* **2015**, *7*, 20623.
19. Jan, K.; Richard, S.; Ivan, H. *J. Polym. Eng.* **2015**, *35*, 21.
20. Sudo, M.; Sumida, K.; Muraki, T.; Kawachi, T.; Kawachi, Y. U.S. Pat. 5,994,465 (**1999**).
21. Resendes, R.; Gronowski, A.; Baba, S.; Seow, Y. S. *Int. Pat. Appl.* WO 2005/080452 A1 (**2005**).
22. Ho, K.; Steevensz, R. *Rubber Chem. Technol.* **1989**, *62*, 42.
23. Takenaka, K.; Suzuki, M.; Takeshita, H.; Miya, M.; Shiomi, T.; Tamamitsu, K.; Konda, T. *J. Polym. Sci. Part A: Polym. Chem.* **2012**, *50*, 659.
24. Flory, P. J. J. *J. Chem. Phys.* **1950**, *18*, 108.
25. Bristow, G. M.; Watson, W. F. *Trans. Faraday Soc.* **1958**, *54*, 1731.
26. Brandrup, J.; Immeraut, E. H. Polymer Handbook; Wiley: New York, **1974**; p 344.
27. Lan, L.; Yinghao, Z.; Yong, Z.; Christopher, O.; Sharon, G. *Appl. Surf. Sci.* **2008**, *255*, 2162.
28. Bokobza, L. *Macromol. Mater. Eng.* **2004**, *289*, 607.
29. Subramani, B. E.; Debdipta, B.; Sankar, R. V.; Burak, K.; Sven, W.; Amit, D.; Kinsuk, N.; Heinrick, G. *J. Appl. Polym. Sci.* **2015**, *132*, DOI: 10.1002/app.41539.
30. Babu, R. R.; Shibulal, G. S.; Chandra, A. K.; Naskar, K. In Advances in Elastomer I; Visakh, P. M., Thomas, S., Chandra, A. K., Mathew, A. P., Eds.; Springer: Berlin, **2013**; p 83.
31. McNeish, J. R.; Parent, J. S.; Whitney, R. A. *Can. J. Chem.* **2013**, *91*, 420.
32. Rana, G.; Catalina, P. B.; Alessandro, G. *Macromolecules* **2002**, *35*, 7246.
33. Nah, C.; Kim, S. G.; Shibulal, G. S.; Yong, H. Y.; Bismark, M.; Byeong, H. J.; Bo, K. H.; Jou, H. A. *Int. J. Hydrogen Energy* **2015**, *40*, 10627.
34. Dluzneski, P. R. *Rubber Chem. Technol.* **2001**, *74*, 451.
35. Kovacic, P.; Hein, R. W. *J. Am. Chem. Soc.* **1959**, *81*, 1190.
36. Baldwin, F. P.; Buckley, D. J.; Kuntz, I.; Robinson, S. B. *Rubber Plast. Age* **1961**, *42*, 500.
37. Kuntz, I.; Zapp, R. L.; Pancirov, R. *J. Rubber Chem. Technol.* **1984**, *57*, 813.